Available online at www.sciencedirect.com
ScienceDirect
Journal of the European Ceramic Society 28 (2008) 871–877
www.elsevier.com/locate/jeurceramsoc

Tantalum doped $0.94Bi_{0.5}Na_{0.5}TiO_3$–$0.06BaTiO_3$ piezoelectric ceramics

Ruzhong Zuo [a,*], Chun Ye [a], Xusheng Fang [a], Jinwang Li [b]

[a] School of Materials Science and Engineering, Hefei University of Technology, Hefei 230009, PR China
[b] Materials and Structures Laboratory, Tokyo Institute of Technology, 4259-R3-20 Nagatsuta, Midori-ku, Yokohama 226-8503, Japan

Received 14 February 2007; received in revised form 31 July 2007; accepted 19 August 2007
Available online 29 October 2007

Abstract

$0.94(Bi_{0.5}Na_{0.5})TiO_3$–$0.06BaTiO_3$ (BNT6BT) ceramics doped with 0–4 mol.% tantalum were investigated in terms of the sintering, microstructure, phase transition, dielectric and piezoelectric properties. Tantalum doping has no remarkable effect on the microstructure and densification within the studied doping content. Up to 4 mol.% tantalum can dissolve into the lattice of BNT6BT ceramics, and the structure symmetry is not changed. However, a significant change in the dielectric behavior and piezoelectric properties took place. With increasing tantalum content, the antiferroelectric phase zone gets broader. Simultaneously, the temperature for a ferroelectric to antiferroelectric phase transition is clearly reduced, and the temperature for a transition from antiferroelectric phases to paraelectric phases is only a bit increased. The results indicate that tantalum occupies B site of a perovskite and behaves as a donor, generating A-site cation vacancies. The properties of the material thus become softer, concerning a reduced coercive field and an improved piezoelectric constant. More than 2 mol.% tantalum doping induces antiferroelectric properties, showing a typical double hysteresis loops, accompanied by a large maximum strain.

Keywords: Sintering; Dielectric properties; Ferroelectric properties; Piezoelectric properties; Lead-free dielectrics; (Bi, Na) TiO_3

1. Introduction

In the last 10 years a remarkable event in the field of piezoelectric materials might be that an increasing attention has been paid to lead-free compositions as a replacement of conventional Pb-based compounds. For example, $Pb(ZrTi)O_3$ ceramics contain at least 70 wt.% of lead oxides and have been commercially applied for almost half a century. They are still main piezoelectric materials so far for various actuator, sensor and transducer applications.[1] These lead-containing materials have been making serious problems to the environment during manufacturing at high temperature or disposal after usage.

A lot of attempts thus have been concentrated on the research and development of high performance lead-free piezoelectric ceramics or single crystals. Bismuth layer (BL) structured and tungsten bronze (TB) type oxides have their own disadvantages over perovskite type ferroelectrics, such as difficult sintering (TB) or electric poling (BL) due to a big structural anisotropy.[2–4] Therefore, perovskite ferroelectrics are usually preferentially chosen as lead-free candidate materials. $Bi_{0.5}Na_{0.5}TiO_3$ (BNT) and $Na_{0.5}K_{0.5}NbO_3$ (NKN) are currently two main lead-free piezoelectric compositions with perovskite structures.[5] Although NKN-based compositions exhibit better piezoelectric and electromechanical properties,[6–8] yet BNT-based lead-free ceramics or single crystals have been commercially used for some applications. The latter possess a relatively mature processing and stable electrical properties. On the contrary, NKN-based compositions show some problems in sintering, control of processing, durability against water, and reproducibility and stability of piezoelectric properties.[5,9–12] Therefore, a lot of things have to be done before the final application.

Since it was discovered by Smolenskii et al. in 1960,[13] BNT has been widely investigated and was considered to be a potential lead-free candidate material. It is a rhombohedral perovskite ferroelectric with a relatively large remnant polarization, $P_r = 38\ \mu C/cm^2$. However, because of its high coercive field, $E_c = 73$ kV/cm, and relatively large conductivity, pure BNT is difficult to be poled and cannot be a good piezoelectric material. These problems were then improved by forming solid solutions with $BaTiO_3$ (BT), $Bi_{0.5}K_{0.5}TiO_3$, $KNbO_3$, $NaNbO_3$, $(Sr_aPb_bCa_c)TiO_3$, $BiFeO_3$, $BiScO_3$, etc.[14–21] Among these systems, BNT-BT seems more interesting. A morphotropic phase

* Corresponding author. Tel.: +86 15955163659; fax: +86 551 2905285.
E-mail address: piezolab@hfut.edu.cn (R. Zuo).

0955-2219/$ – see front matter © 2007 Elsevier Ltd. All rights reserved.
doi:10.1016/j.jeurceramsoc.2007.08.011

boundary (MPB) was found out in this system at ~6 mol.% BT, where the materials show enhanced dielectric, piezoelectric and electromechanical performances. Takenaka et al. reported that 0.94BNT–0.06BT ceramics have relatively good properties of $k_{33} = 0.55$, $k_{31} = 0.19$, $d_{33} = 125$ pC/N and $d_{31} = 40$ pC/N.[15] These properties were afterwards promoted by a few research groups.[22–24] However, this material system has a higher coercive electric field and medium piezoelectric constants. It was believed that aliovalent substitution at A site or B site may induce soft or hard properties in a piezoelectric material by forming cation vacancies or oxygen vacancies, respectively. Several kinds of cations like La^{3+}, Nb^{5+}, Co^{3+}, Mn^{2+}, etc. were tested to further modify BNT-based lead-free piezoelectric ceramics.[25–28]

In this study, a small amount of tantalum was used to modify 0.94BNT–0.06BT compositions which are near the MPB of this system. The influence of tantalum addition on the microstructure, dielectric behavior, and piezoelectric responses was discussed.

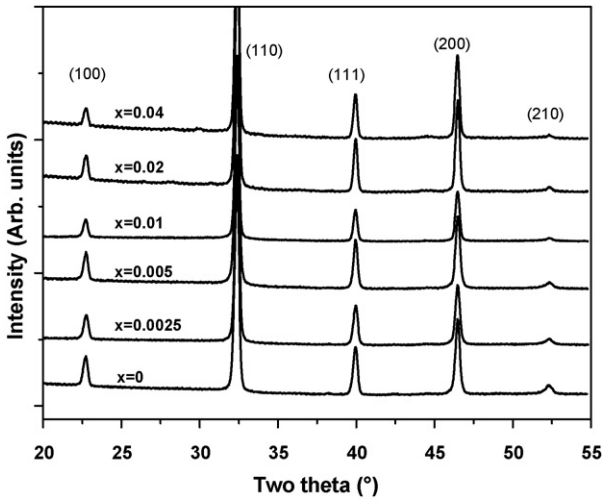

Fig. 1. X-ray diffraction patterns of $(1-x)$(0.94BNT–0.06BT)–xTa ceramics.

2. Experimental procedure

A conventional mixed oxide route was utilized to prepare $(1-x)$(0.94BNT–0.06BT)–xTa ceramics (abbreviated as BNT6BTx, $x = 0$, 0.0025, 0.005, 0.01, 0.02, and 0.04). The starting raw materials are high purity oxides or carbonates, Bi_2O_3 (99.97% in purity), TiO_2 (99.9%), Na_2CO_3 (99.9), $BaCO_3$ (99.8%). Tantalum was added in its oxide form, Ta_2O_5 (99.0%). First of all, all powders for 0.94BNT–0.06BT compositions were weighed and put in a nylon jar together with anhydrous ethanol as the medium, following a planetary ball milling process for 18 h. The dried powder mixtures were calcined at 820 °C for 4 h. The calcined BNT6BT powder was divided into six pieces. Ta_2O_5 was added into each piece according to its doping content. After that, the powders were mixed for 24 h again in a planetary ball mill to ensure a good distribution of the dopant, and to reduce the particle size for better densification as well. The dried powders sieved through 230 meshes were compacted into disk specimens under a uniaxial pressure of ~50 MPa. No binder was used in this step. Sintering was carried out in air on a platinum foil in the temperature range of 1100–1200 °C for 1–4 h at a heating rate of 300 °C/h.

The microstructure of the sintered samples was observed by a scanning electron microscope (SEM, Philips Electronic Instruments). The Archimedes method was used to measure the density of each sintered specimen. A powder X-ray diffractometer (XRD, Rigatu) was utilized to identify the crystalline structures using a Cu Kα radiation.

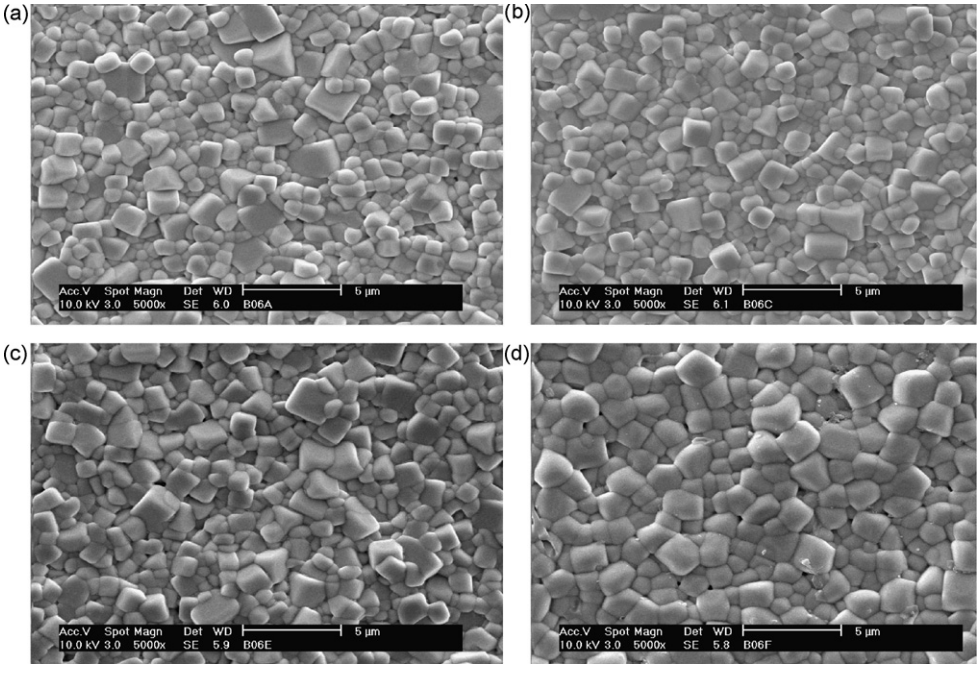

Fig. 2. SEM images of $(1-x)$(0.94BNT–0.06BT)–xTa ceramics sintered at 1150 °C for 2 h: (a) $x = 0$, (b) $x = 0.005$, (c) $x = 0.02$, (d) $x = 0.04$.

Silver paste was fired on two major surfaces of each specimen as electrodes after a careful polishing process. Simultaneously, the sample thickness was reduced by polishing it to reach an aspect ratio of 0.1 for a good measurement of electromechanical coupling properties. The dielectric properties as a function of temperature and frequency were obtained by an impedance analyzer (HP4284). Polarization and strain hysteresis loops were measured in a silicone oil bath by applying an ac field at a frequency of 300 mHz by means of a modified Sawyer–Tower bridge. The piezoelectric constants d_{33} and the planar electromechanical coupling factor k_p were measured only 24 h after a poling process. The sample was poled in a silicone oil bath with a programmable temperature controller under a dc field of 3–6 kV/mm for 20–30 min. The poling temperature was in the range of 25–120 °C. A quasistatic Berlincourt meter was used to measure d_{33}. The k_p value was obtained by a resonance-antiresonance method through an impedance analyzer (HP4192A) on the basis of IEEE standards.

3. Results and discussion

Fig. 1 shows the crystalline structure of BNT6BTx compositions synthesized at 1150 °C. It is clear that all compositions exhibit typical ABO_3 perovskite diffraction peaks with a rhombohedral symmetry. No trace of secondary phases is detectable, meaning that all doped tantalum ions have dissolved into the lattice of BNT6BT. Small lattice shrinkage caused by vacancies of A site cations, if Ta^{5+} occupies Ti^{4+} at B site, was not detected by XRD. This is probably due to a compensation of the lattice expansion from the substitution of Ta^{5+} for Ti^{4+} ($R_{Ta} = 0.64$ Å, $R_{Ti} = 0.61$ Å).[29] Fig. 2 shows the microstructure of BNT6BT ceramics doped with different concentrations of tantalum sintered at 1150 °C for 2 h. All samples have dense microstructures, with an average grain size of 1.7 μm. The Archimedes method gave a relative density of more than 96% of the theoretical values for all samples. However, tantalum doping has a little influence on the sintering of BNT6BT

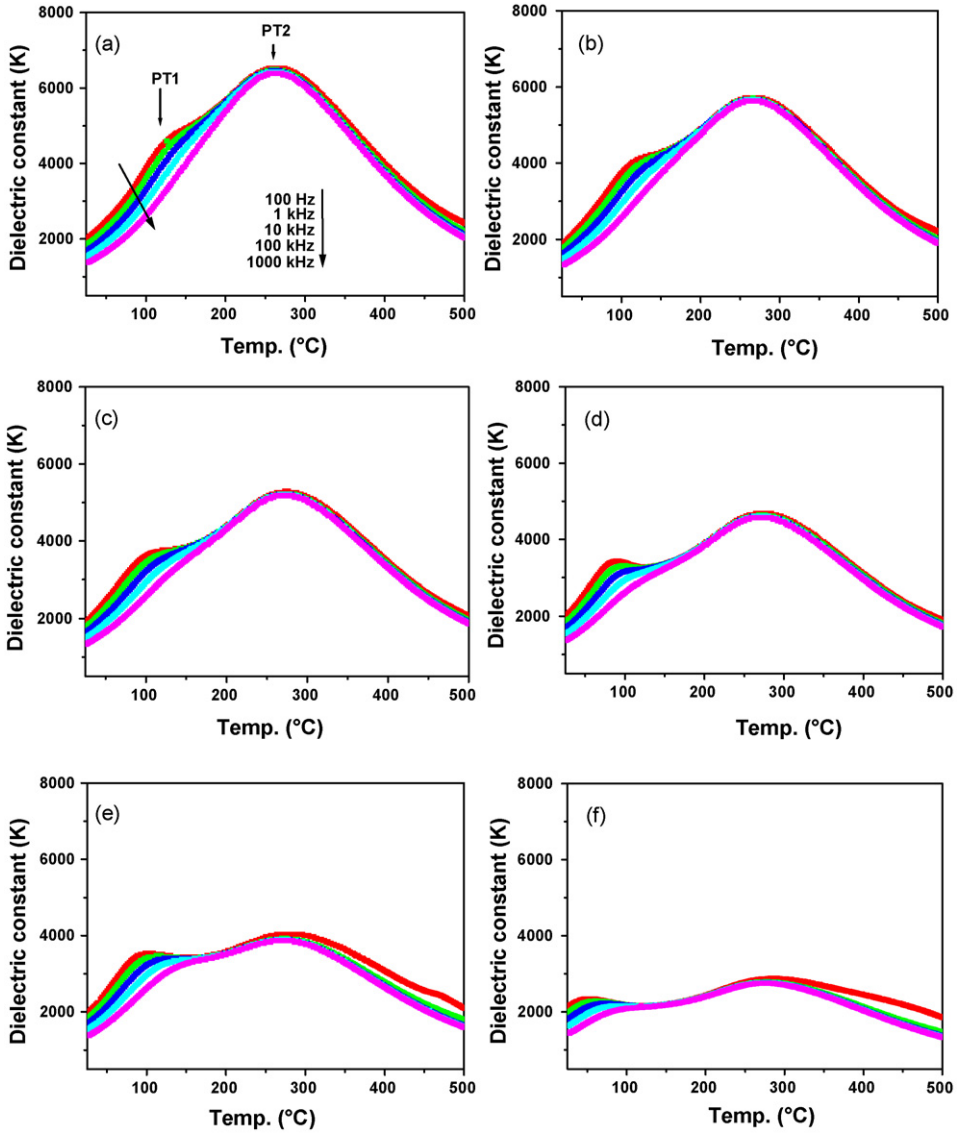

Fig. 3. Dielectric constants of $(1-x)$(0.94BNT–0.06BT)–xTa ceramics as a function of temperature and frequency: (a) $x = 0$, (b) $x = 0.0025$, (c) $x = 0.005$, (d) $x = 0.01$, (e) $x = 0.02$ and (f) $x = 0.04$.

ceramics and the grain growth was not evidently affected as well.

The dielectric properties of BNT6BTx ceramics as a function of temperature and frequency are shown in Fig. 3. The curves for different samples look similar, all showing two-phase transitions, as indicated in Fig. 3a. One is diffuse at lower temperature and another is normal at high temperature. This feature intrinsically comes from pure BNT which was reported to have a diffuse structural phase transition from rhombohedral ferroelectrics to tetragonal antiferroelectrics at ~200 °C and a Curie phase transition from the antiferroelectric to paraelectric phases at ~320 °C.[13] BNT6BT ceramics may show similar phase transition behavior, as confirmed by the phase diagram of BNT-BT.[15] However, a clear difference was made by tantalum doping. First of all, with doping more tantalum, the dielectric maxima become significantly lower. It is ~7000 for pure BNT6BT and only 3000 for 4 mol.% tantalum doped BNT6BT. Accordingly, the curves become flatter and the dielectric constants show lower and lower temperature dependence. Tantalum seems to act as a suppressor. Secondly, the temperature for the first phase transition (PT1) gradually shifts to lower temperature with doping tantalum. However, the second phase transition (PT2) temperature seems to change not much. This implies that tantalum doping makes the antiferroelectric zone larger and more stable. For 1 mol.% and 2 mol.% tantalum doped samples, PT1 lies slightly above room temperature. Moreover, the phase transition for these two samples looks quite similar in terms of the diffusivity and the location, but the dielectric maxima conform to the normal tendency with tantalum doping. When 4 mol.% tantalum is doped, the PT1 temperature gets very close to room temperature, but the material still has a rhombohedral symmetry as confirmed by XRD in Fig. 1. Finally, the peak (dielectric anomaly) for the first phase transition gets more and more visible with doping more tantalum. It is only a "shoulder" for pure BNT6BT and however becomes a distinct peak for 1 mol.% tantalum doped BNT6BT. Fig. 4 presents a direct comparison of the dielectric-temperature curves at a frequency of 1 kHz for BNT6BTx ceramics. The temperature for the dielectric maxima, T_{max}, gets slightly increased with doping tantalum. By comparison, the temperature for PT1, T_{sec}, was clearly altered by tantalum doping. Fig. 4b shows that the dielectric loss has not much change at room temperature, but it gets lower near T_{sec} with increasing tantalum-doping content.

The polarization vs. electric field hysteresis loops for all samples was measured, as shown in Fig. 5. It is evident that tantalum doping has a big effect on the ferroelectric properties of BNT6BT samples. The remnant polarization, P_r, and the coercive field, E_c, become lower due to doping a small amount of tantalum. A big change takes place when more than 1 mol.% tantalum is doped. The 2 mol.% tantalum doped BNT6BT samples show double hysteresis loops typical for an antiferroelectric. Compared to 4 mol.% tantalum doped BNT6BT samples, the antiferroelectric states in 2 mol.% tantalum doped BNT6BT samples are closer to the ferroelectric states in energy; thereby there is a smaller forward switching electric field. Therefore, the 4 mol.% tantalum doped BNT6BT ceramics exhibit only a linear relationship between the electric field and the polarization due to the field effect of a dielectric (dielectric polarization). The corresponding strain "butterfly" loops are shown in Fig. 6. The pure electrostrictive effect is the cause of Fig. 6f. Fig. 6e is a strain vs. electric field loop typical for an antiferroelectric, which has no any remnant strain. Noticeably, the 1 mol.% tantalum doped BNT6BT samples show the largest the maximum strain S_{max} (~0.4%) and the remnant strain S_r (0.21%) among all samples. Their coercive fields are clearly reduced. It can be expected that tantalum dopant behaviors as a "donor" in BNT6BT matrix compositions, probably generating vacancies of A-site cations. The soft properties are thus induced, concerning a reduced E_c and an improved d_{33}. When the doping content of tantalum reaches 2 mol.%, the material becomes antiferroelectric, showing typical double hysteresis loops. Unfortunately, its forward switching electric field is as high as 5.2 kV/mm, so that the maximum strain (3.6% currently) is not yet reached under a driving electric field of 6 kV/mm. One thing is worth of note that 2 mol.% or 4 mol.% tantalum doped BNT6BT compositions show antiferroelectric behavior (Figs. 5 and 6), but have a rhombohedral symmetry (see Fig. 1), rather than a tetragonal symmetry. This is probably due to the diffuse feature of the first phase transition.

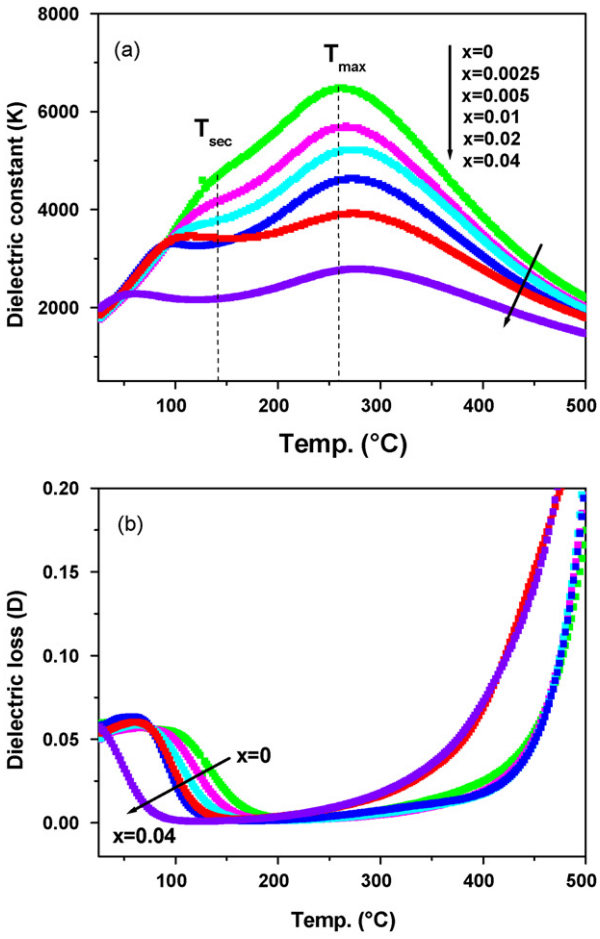

Fig. 4. Dielectric constants (a) and losses (b) at a frequency of 1 kHz of $(1-x)$(0.94BNT–0.06BT)–xTa ceramics as a function of temperature.

Table 1 collects various room-temperature properties of BNT6BTx ceramics sintered at 1150 °C for 2 h. The sample density and room temperature dielectric properties are not sig-

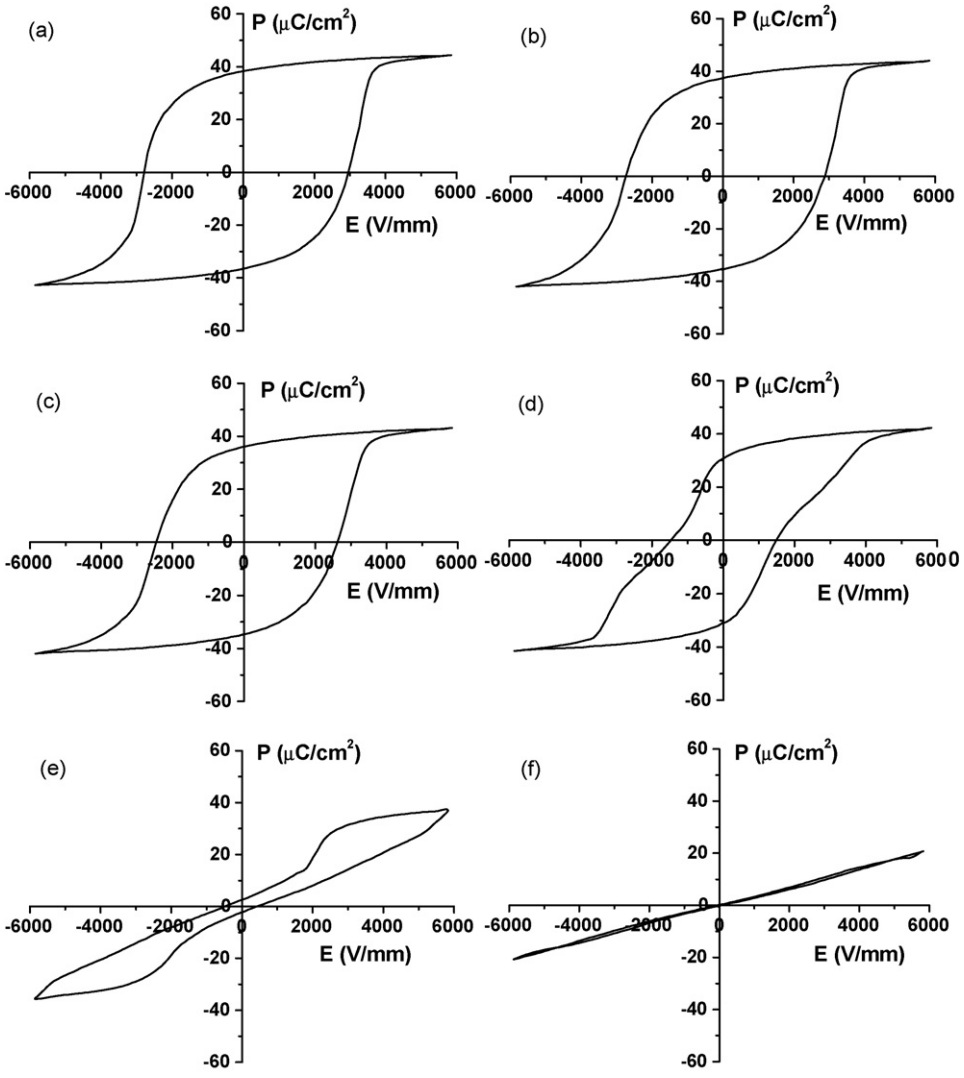

Fig. 5. Polarization vs. electric field hysteresis loops of $(1-x)$(0.94BNT–0.06BT)–xTa ceramics: (a) $x=0$, (b) $x=0.0025$, (c) $x=0.005$, (d) $x=0.01$, (e) $x=0.02$ and (f) $x=0.04$.

nificantly changed. The dielectric losses are increased very little. The temperature for two-phase transitions is altered with increasing tantalum concentration. There is a slight increase for T_{max}, but a remarkable reduction for T_{sec}. The piezoelectric constant is gradually increased and reaches the best value of 171 pC/N at the doping level of 1 mol.% tantalum. The electromechanical coupling factor, k_p, has a little vibration. A small d_{33} for 2 mol.% tantalum doped BNT6BT may be from the remnant ferroelectric polarization after it was cycled under the ac field of 6 kV/mm. However, this composition has a quite large S_{max} value from an electric field driven antiferroelectric–ferroelectric phase transition, without any hysteresis. Tantalum doped BNT6BT antiferroelectric compositions may be also interesting for an actuator application if the doping level can be slightly adjusted to modify the phase switching characteristic.

Table 1
Room temperature dielectric properties and piezoelectric responses of $(1-x)$(0.94BNT–0.06BT)–xTa ceramics

	$x=0$	$x=0.0025$	$x=0.005$	$x=0.01$	$x=0.02$	$x=0.04$
Density (g/cm^3)	5.82	5.83	5.82	5.83	5.85	5.86
K (1 kHz)	1846	1762	1784	1861	1847	1985
tan δ (1 kHz) (%)	5.03	4.99	5.03	5.84	5.36	5.73
d_{33} (pC/N)	155	156	170	171	15	–
k_p (%)	35.4	35.4	35.9	33.0	–	–
T_{sec} (°C) (1 kHz)	126	114	103	89	94	58
T_{max} (°C)	263	264	269	273	275	278

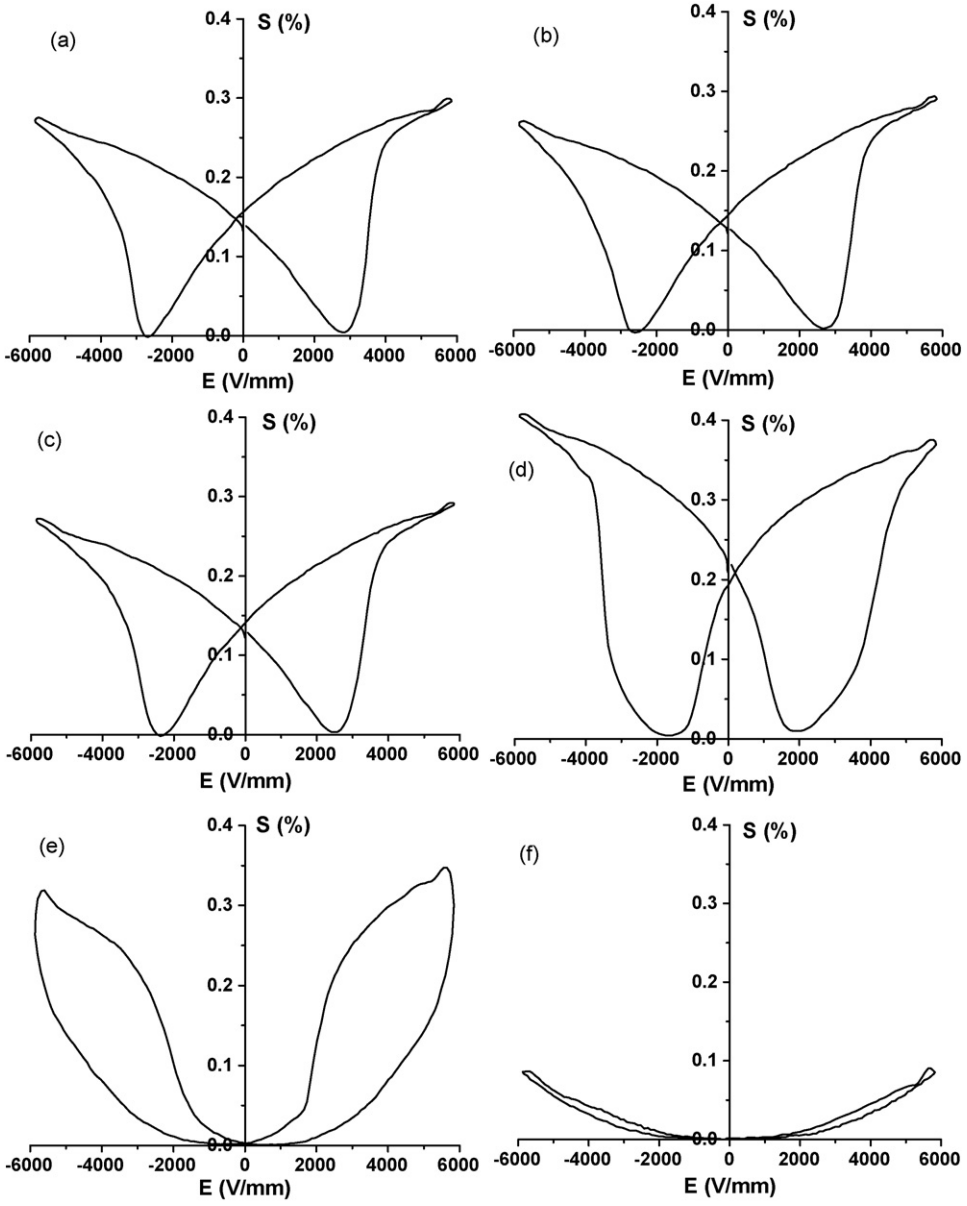

Fig. 6. Strain vs. electric field butterfly loops of $(1-x)$(0.94BNT–0.06BT)–xTa ceramics: (a) $x=0$, (b) $x=0.0025$, (c) $x=0.005$, (d) $x=0.01$, (e) $x=0.02$ and (f) $x=0.04$.

4. Conclusions

Tantalum doped 0.94BNT–0.06BT lead-free piezoelectric ceramics have been prepared by a conventional mixed oxide route. The influence of tantalum addition on the microstructure and various electric properties was investigated. A small amount of tantalum doping up to 4 mol.% does not significantly affect the sintering and microstructure. Due to the occupation of tantalum on B site as a donor, the material properties thus get softer electrically. The piezoelectric constants are slightly improved; however, the desirable working temperature for a piezoelectric ceramic is reduced. More than 2 mol.% tantalum doping induces antiferroelectric properties in the material by broadening the antiferroelectric phase area.

Acknowledgements

Financial supports from HFUT RenCai Foundation (103–035006) and a special Program for Excellence Selection "R & D of Novel Lead-Free Piezoelectric Ceramics" (103–035034) are greatly acknowledged.

References

1. Jaffe, B., Cook, W. R. and Jaffe, H., *Piezoelectric Ceramics*. Academic Press, New York, 1971, pp. 115–181.
2. Suzuki, M., Nagata, H., Ohara, J., Funakubo, H. and Takenaka, T., $Bi_{3-x}M_xTiTaO_9$ (M = La or Nd) ceramics with high mechanical quality factor Qm. *Jpn. J. Appl. Phys.*, 2003, **42**, 6090–6093.
3. Sawada, T., Ando, A., Sakabe, Y., Damjanovic, D. and Setter, N., Properties of the elastic anomaly in $SrBi_2Nb_2O_9$-based ceramics. *Jpn. J. Appl. Phys.*, 2003, **42**, 6094–6098.

4. Xie, R. J., Akimune, Y., Wang, R., Hirosaki, N. and Nishimuna, T., Dielectric and piezoelectric properties of barium-substituted $Sr_{1.9}Ca_{0.1}NaNb_5O_{15}$ ceramics. *Jpn. J. Appl. Phys.*, 2003, **42**, 7404–7409.
5. Maeder, M. D., Damjanovic, D. and Setter, N., Lead free piezoelectric materials. *J. Electroceram.*, 2004, **13**, 385–392.
6. Guo, Y., Kakimoto, K. and Ohsato, H., Phase transitional behavior and piezoelectric properties of $Na_{0.5}K_{0.5}NbO_3$–$LiNbO_3$ ceramics. *Appl. Phys. Lett.*, 2004, **85**, 4121–4123.
7. Saito, Y., Takao, H., Tani, T., Nonoyama, T., Takatori, K., Homma, T., Nagaya, T. and Nakamura, M., Lead free piezoceramics. *Nature*, 2004, **432**, 84–87.
8. Hollenstein, E., Davis, M., Damjanovic, D. and Setter, N., Piezoelectric properties of Li- and Ta-modified $K_{0.5}Na_{0.5}NbO_3$ ceramics. *Appl. Phys. Lett.*, 2005, **87**, 182905.
9. Matsubara, M., Yamaguchi, T., Kikuta, K. and Hirano, S., Sinterability and piezoelectric properties of (K,Na)NbO_3 ceramics with novel sintering aid. *Jpn. J. Appl. Phys.*, 2004, **43**, 7159–7163.
10. Kosec, M. and Kolar, D., On activiated sintering and electrical properties of $NaKNbO_3$. *Mater. Res. Bull.*, 1975, **10**, 335–340.
11. Zeyfang, R. R., Henson, R. M. and Maier, W. J., Temperature- and time-dependent properties of polycrystalline (Li,Na)NbO_3 solid solutions. *J. Appl. Phys.*, 1977, **48**, 3014–3017.
12. Yoo, J., Lee, K., Chung, K., Lee, S., Kim, K., Hong, J., Ryu, S. and Lhee, C., Piezoelectric and dielectric properties of (LiNaK)(NbTaSb)O_3 ceramics with variation in poling temperature. *Jpn. J. Appl. Phys.*, 2006, **45**, 7444–7448.
13. Smolenskii, G. A., Isupov, V. A., Agranovskaya, A. I. and Krainik, N. N., New ferroelectrics of complex composition. *Sov. Phys.-Solid State (Engl. Transl.)*, 1961, **2**, 2651–2654.
14. Takenaka, T., Sakata, K. and Toda, K., Piezoelectric properties of $(Bi_{0.5}Na_{0.5})TiO_3$-based ceramics. *Ferroelectrics*, 1990, **106**, 375–380.
15. Takenaka, T., Maruyama, K. and Sakata, K., $(Bi_{0.5}Na_{0.5})TiO_3$–$BaTiO_3$ system for lead free piezoelectric ceramics. *Jpn. J. Appl. Phys.*, 1991, **30**, 2236–2239.
16. Nagata, H. and Takenaka, T., Lead free piezoelectric ceramics of $(Na_{0.5}Bi_{0.5})TiO_3$–$1/2(Bi_2O_3{\cdot}Sc_2O_3)$ system. *Jpn. J. Appl. Phys. Part 1*, 1997, **36**, 6055–6057.
17. Nagata, H. and Takenaka, T., Lead-free piezoelectric ceramics of $(Bi_{0.5}Na_{0.5})TiO_3$–$KNbO_3$–$1/2(Bi_2O_3{\cdot}Sc_2O_3)$ system. *Jpn. J. Appl. Phys.*, 1998, **37**, 5311–5314.
18. Sasaki, A., Chiba, T., Mamiya, Y. and Otsuki, E., Dielectric and piezoelectric properties of $(Bi_{0.5}Na_{0.5})TiO_3$–$(Bi_{0.5}K_{0.5})TiO_3$ systems. *Jpn. J. Appl. Phys.*, 1999, **38**, 5564–5567.
19. Nagata, H., Koizumi, N. and Takenaka, T., Lead-free piezoelectric ceramics of $(Bi_{0.5}Na_{0.5})TiO_3$–$BiFeO_3$ system. *Key Eng. Mater.*, 1999, **169–170**, 37–40.
20. Wada, T., Toyoike, K., Imanaka, Y. and Matsuo, Y., Dielectric and piezoelectric properties of $(A_{0.5}Bi_{0.5})TiO_3$–$ANbO_3$ (A = Na, K) systems. *Jpn. J. Appl. Phys.*, 2001, **40**, 5703–5705.
21. Li, Y. M., Chen, W., Xu, Q., Zhou, J., Sun, H. J. and Liao, M. S., Dielecric and piezoelectric properties of $Na_{0.5}Bi_{0.5}TiO_3$–$K_{0.5}Bi_{0.5}TiO_3$–$NaNbO_3$ lead free ceramics. *J. Electroceram.*, 2005, **14**, 53–58.
22. Wu, Y. G., Zhang, H. L., Zhang, Y., Ma, J. Y. and Xie, D. H., Lead free piezoelectric ceramics with composition of $(0.97-x)Na_{0.5}Bi_{0.5}TiO_3$–$0.03NaNbO_3$–$xBaTiO_3$. *J. Mater. Sci.*, 2003, **38**, 987–994.
23. Nagata, H., Yoshida, M., Makiuchi, Y. and Takenana, T., Large piezoelectric constant and high Curie temperature of lead-free piezoelectric ceramic ternary system based on bismuth sodium titanate-bismuth potassium titanate-barium titanate near the morphotropic phase boundary. *Jpn. J. Appl. Phys.*, 2003, **42**, 7401–7403.
24. Wu, L., Xiao, D. Q., Lin, D. M., Zhu, J. G. and Yu, P., Synthesis and properties of $Bi_{0.5}(Na_{1-x}Ag_x)_{0.51-y}Ba_yTiO_3$ piezoelectric ceramics. *Jpn. J. Appl. Phys.*, 2005, **44**, 8515–8518.
25. Herabut, A. and Safari, A., Processing and electromechanical properties of $(Bi_{0.5}Na_{0.5})_{(1-1.5x)}La_xTiO_3$ ceramics. *J. Am. Cearm. Soc.*, 1997, **80**, 2954–2958.
26. Li, H. D., Feng, C. D. and Xiang, P. H., Electrical properties of La^{3+} doped $(Na_{0.5}Bi_{0.5})_{0.94}Ba_{0.06}TiO_3$ ceramics. *Jpn. J. Appl. Phys.*, 2003, **42**, 7387–7391.
27. Li, H. D., Feng, C. and Yao, W., Some effects of different additives on dielectric and piezoelectric properties of $(Bi_{1/2}Na_{1/2})TiO_3$–$BaTiO_3$ morphotropic phase boundary composition. *Mater. Lett.*, 2004, **58**, 1194–1198.
28. Zhou, X., Gu, H. S., Wang, Y., Li, W. Y. and Zhou, T. S., Piezoelectric properties of Mn-foped $(Na_{0.5}Bi_{0.5})_{0.92}Ba_{0.08}TiO_3$ ceramics. *Mater. Lett.*, 2005, **59**, 1649–1652.
29. Shannon, R. D., Revised effective ionic radii and systematic studies of interatomie distances in halides and chaleogenides. *Acta Cryst.*, 1976, **A32**, 751–767.